Asian Journal of
Science, Technology, Engineering, and Art

e-ISSN: 3025-4507
p-ISSN: 3025-5287
Index: Harvard, Boston, Sydney University, Dimensions, Lens, Scilit, Semantic, Google, etc

https://doi.org/10.58578/AJSTEA.v4i1.8548

Design of Reference Model Adaptive Based Discrete-Time PID Controller for Satellite Yaw-Axis Attitude Control System

Emmanuel E. Egwim[1], Ikemsinachi Chikeziri Osuagwu[2], Nnanyereugo Nnamdi Emeribe[3]
[1]Bells University of Technology, Ota, Nigeria; [2]Chukwuemeka Odumegwu Ojukwu University, Uli, Nigeria; [3]Imo State University, Owerri, Nigeria
emmanuel.egwim@yahoo.com; ikemsinachilove@gmail.com

Article Info:

Submitted:	Revised:	Accepted:	Published:
Dec 24, 2025	Feb 15, 2026	Feb 5, 2026	Feb 23, 2026

Abstract

Effective satellite attitude control systems are essential to ensure both the quality and reliability of data acquisition in microsatellites. This paper presents the design and performance analysis of an adaptive controller for a microsatellite yaw-axis (y-axis) attitude control system (ACS). The transfer function models of the amplifier, actuator, and satellite structure were first derived to obtain the overall transfer function of the microsatellite yaw-axis attitude dynamics. Based on these models, a Model Reference Adaptive Control–based Discrete-Time Proportional–Integral–Derivative controller (MRAC-DPID) was designed and integrated into the closed-loop network of the microsatellite yaw-axis ACS. A computer-based MATLAB/Simulink model was then developed using the mathematical representation of the closed-loop system, and simulations were conducted to evaluate the attitude response under the MRAC-DPID controller. The simulation results demonstrate that the proposed MRAC-DPID significantly improves both transient and steady-state performance, as reflected in reduced rise time, settling time, overshoot, and steady-state error. Overall, the controller satisfies all specified performance criteria and provides the best step-response performance with respect to overshoot for adaptation gains in the range of 0.1 to 1. The study concludes

AJSTEA Journal is licensed under a Creative Commons Attribution-NonCommercial-ShareAlike 4.0 International License

that the MRAC-DPID controller offers an effective adaptive control strategy for microsatellite yaw-axis attitude regulation, thereby supporting improved stability and reliability of microsatellite operations.

Keywords: Attitude Control System; Microsatellite; Model Reference Adaptive Control; Discrete-Time PID Controller; Yaw-Axis Attitude Control

INTRODUCTION

The critical demand for high-precision satellite attitude control is increasing, and the needs for reliable, stable and accurate satellite control system are becoming increasingly stringent considering the rapid development in aerospace industry. The flight attitude of a satellite will change due to varying angular variations in pitch, yaw, and roll caused by gravitational perturbation and external disturbance during the on-orbit flight of the satellite. Considering, most specifically, the fact that some satellites have defined observation tasks, the slight change of attitude angle of satellite through the orbit radius enlargement with respect to the displacement deviation cannot be neglected. Since the performance of satellite tasks are directly determined by the control effect, it is of critical concern to investigate attitude control system and choose the control technique that will give better transient and steady-state performance for microsatellite. Many of the studies on satellite attitude control have used Proportional-Integral-Derivative (PID) controller, which is example of linear control system. However, PID controller suffers from the effect of disturbance or change in system dynamic parameters.

As result of the critical demand for high-precision Satellite Attitude Control (SAC), several control techniques have been designed to meet certain performance criteria for better stability and accuracy in satellite attitude tracking. A satellite in its on-orbit flight will experience pitch, yaw, and roll variations because of external disturbances and gravitational influence. The effect of the action of these disturbances on the satellite can result in its displacement over time and as such resulting to the angular variation in pitch, yaw and roll (Travis, 2020). Thus, it is important to have a subsystem that provides the needed manoeuvring to ensure that an on-orbit flight satellite is maintained at a predetermined position and a defined attitude in order to achieve expected task and meet designed specifications or performance standards. On account of this, satellite attitude control system (SACS) is integrated with a controller that serves as the subunit providing the

needed manoeuvring capacity to keep the satellite in its defined orientation for effective flight operation. However, to effectively accomplish its tasks, it is critical to study the satellite's control subsystem in order to choose the appropriate control algorithm that offers improved dynamic or transient behaviour and steady-state performance for flight attitude adjustment and stability.

Considering the fact that attitude angles of a satellite can be put out of place due to various sources of natural disturbance such as the radiation pressure from solar, gravity gradient of the earth, and the magnetic field of the Earth; and because successful mission of a satellite depends on its ability to maintain a predetermined orientation with respect to the Earth (Nobari, 2013), several control schemes have been developed for stabilizing attitude motion. For instance, attitude control functions were provided by the attitude and control subsystem (ADCS) together with de-tumbling and satellite angular velocity stabilization and in addition to the orbit and attitude information estimation during the operation of a microsatellite satellite using unscented Kalman filter (UKF) (Shou, 2014). PID controller was designed using the Ziegler-Nichols tuning method and it was introduced into the closed loop of satellite model for the determination and control of yaw-axis in Mbaocha *et al.* (2016). Similarly, Hassan (2009) used PID controller in satellite attitude control system to achieve rapid settling time, reduced overshoot and zero steady-state error. A fourth order microsatellite system was approximated by its second order version and used for design of ITAE based PID controller for stabilizing attitude motion for microsatellite yaw-axis (Ajiboye *et al.*, 2020). The kinematic model and dynamic model of satellite attitude were established together PID controller and fuzzy-PID controller designed to carry out digital simulation of the SAC developed based on the mathematical model of satellite attitude (Shan *et al.*, 2022). In the same vein, classical PD controller was replaced with FLC for yaw-axis closed loop reaction wheel of LEO microsatellite attitude stabilization (Benzeniar & Fellah, 2014). In Portella *et al.* (2020) the performance of a satellite in a circular orbit with four control moment gyroscopes (CMGs) in pyramidal configuration was investigated either by employing Exponential Mapping Control (EMC) or Linear Quadratic Tracker (LQT) with integral compensator. Bello *et al.* (2023) designed fuzzy Logic Controller (FLC), conventional PID controller, and adaptive PID controller that uses logic blocks that resets (or zeroes) the integral element whenever change of sign in error function occurs were experimentally compared in a laboratory nanosatellite and its testing system with the results showing that using FLC rather than PID yielded significant

improvement in energy consumption, convergence time and robustness in accordance to changes in environmental condition, which were the performance criteria including steady state error (accuracy). Attitude stabilization was achieved using a reaction and two magnetic torquers with a multiple-input multiple-output (MIMO) fuzzy logic feedback algorithm for attitude control system (Shahmohamadi & Rezaeiha, 2012). Narkiewicz *et al.* (2020) used selectable gains PID controllers for a generic model of a nanosatellite attitude control and stabilization system whose performance was evaluated in three modes of operations namely, de-tumbling after isolation from the launcher, nominal operation when the satellite attitude is subjected to slight or moderate perturbation, and momentum unloading following reaction wheel saturation. In the study carried out by Jin and Li (2022), three-axis stabilization control and pointing stabilization control of under-actuated spacecraft attitude with two reaction wheels was achieved using an integrated control technique based on dual-mode Model Predictive Control (MPC) and utilizing solar radiation pressure from two solar panels. Improvement of convergence rate for attitude control of satellites was achieved using variable structure PID controller, which integrates the classical PID algorithm, trajectory panning, variable structure and fault tolerance in Qi *et al.* (2022). An attitude determination and control system (ADCS) was developed for a satellite using Direct Torque Control (DTC) based scheme that uses PID algorithm to compute the demand torque to actuator from the error between the desired attitude and estimated attitude and followed by DTC on the actuator for stabilizing pitch, roll and yaw angles of satellite ACS was implemented in Dass *et al.* (2019). Control system for tracking of satellite attitude was achieved using control algorithm based on Lyapunov stability control theory in Okasha *et al.* (2019).

Classical PID controllers have been largely employed in many studies relating to satellite attitude control system and design simplicity including the ability to provide control effort for system with complex dynamics generally in several industrial process control operations because of its associated simple structure. In nanosatellite ACS, PID controllers shown weakness of relatively long area of little variation phase prior to correcting the final sate in some manoeuvres and was unable to stabilize LEO satellite attitude after 500 s which is beyond allowable practical value (Bello *et al.*, 2023; Enejor *et al.*, 2023). Intelligent based control such as FLC and fuzzy-PID have been proposed to replace PID controllers. This can be attributed to the fact that heuristic information is used by FLC to offer realistic and expedient alternative to addressing nonlinear problems related to

control systems (Eze *et al.*, 2021). However, the use of FLC controller only results in steady-state error (Agwah & Eze, 2022) while expert PID and fuzzy-PID controllers on the other hands, always have sub-par timing precision and limited anti-interference capabilities (Liu *et al.*, 2023). Even though CMGs are satellite attitude control actuators that act as torque amplifier and suitable for three-axis slew manoeuvring, the drawback of the scheme is the possibility of singularities for certain gimbal angles combination (Si Mohammed, 2012). LQR and LQG controllers have the ability to provide optimal control to system performance with improved settling time and almost zero overshoot (or oscillation), but their feat degrades because of nonlinearity and delay as the system reaches the setpoint (Eze *et al.*, 2021). Also, similar to PID controller, the gain matrices of LQG and LQR are fixed and could be influenced by parameter variation (Eze & Ezenugu, 2024; Eze, Obichere, Mbonu, & Onojo, 2024).

Thus, in this work, the goal is to meet the design specifications of a microsatellite yaw-axis ACS while reducing pointing (or position) deviation or error to zero with improved system stability and ensuring that the orientation accuracy is maintained using model reference adaptive control (MRAC) based discrete time PID controller with that is capable of providing a suitable unique adaption potential via a wide range of adaption gain to on-orbit flight satellite with respect to yaw angle stabilization.

System Design and Specifications

System modelling

The closed loop description of a microsatellite yaw-axis ACS studied in Ajiboye et al. (2020) is shown in Figure 1. It is a Single Input Single Output (SISO) linear time-invariant (LTI) system with unity feedback gain. With the block diagram arrangement, the microsatellite yaw-axis ACS can be vividly described in very simplified manner. Thus, as shown in Figure 1, during the on-orbit flight of the satellite, an attitude manoeuvre takes place which involves the controller sending a control signal to the amplifier in order to boost the signal strength (via increase in magnitude) and the amplified signal (which is the motor armature voltage) reaches the actuator (motor) that produces a proportional output that is sufficient enough to adjust the satellite structure (plant) orientation in terms of yaw angle in this case according to the error signal (which is the difference between the desired (target) attitude and the actual attitude measured by the feedback sensor. Generally, the

attitude controller is designed to align the actual attitude (yaw angle) to a desired attitude (or target angle). The desired attitude can be pointing in fixed direction (that is static orientation) or dynamic with respect to time (Bello *et a*l., 2023).

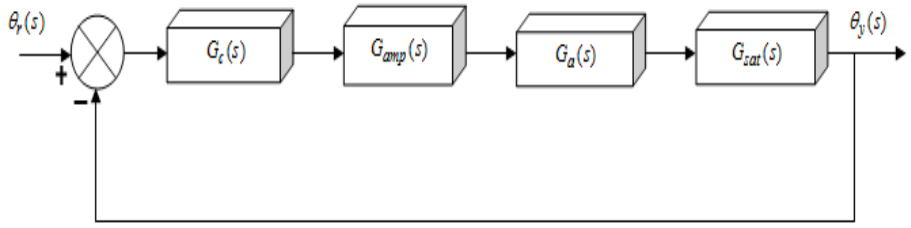


Figure 1. Block diagram of attitude control loop

The dynamics of the amplifier, actuator and the satellite structure are determined in terms of transfer functions in Laplace form (s-domain) given by Ajiboye *et al.* (2020):

$$G_{sat}(s) = \frac{1}{0.8\,s^2} \quad (1)$$

$$G_a(s) = \frac{78.3\,s}{s^2+1815.4\,s+24466} \quad (2)$$

$$G_{amp}(s) = \frac{240}{0.1\,s+1} \quad (3)$$

where$G_{sat}(s)$ is the satellite structure (plant) dynamic, $G_a(s)$ is the actuator dynamic, and $G_{amp}(s)$ is the amplifier dynamic. The MATLAB/Simulink model of the system (without controller) regarding Equations (1) to (3) is shown in Figure 2.

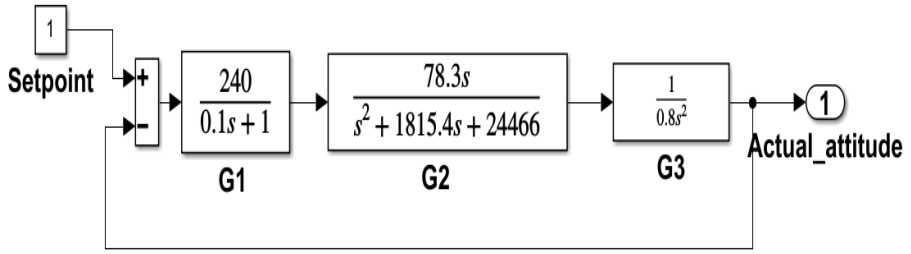


Figure 2. System model without controller in MATLAB/ Simulink

The system will hence forth be evaluated in state space form rather than transfer function. This is because to design a LQR, the system has to be represented in state space form. The cascade combination of Equations (1) to (3) gives the forward path gain expressed in Equation (4) for the closed loop system in Figure 1 neglecting the controller. Substituting the numerical values of the transfer functions and using software (i.e., MATLAB) to compute Equation (4) gives Equation (5).

$$G(s) = G_{amp}(s) \times G_a(s) \times G_{sat}(s) \quad (4)$$

$$G(s) = \frac{18792\,s}{0.08\,s^5 + 146\,s^4 + 3410\,s^3 + 1.957\times10^4 s^2} \quad (5)$$

Equation (5) shows that the overall dynamic for yaw-axis attitude determination for the microsatellite is 5th order system considering the individual component (amplifier, actuator and satellite structure) transfer function. Thus, using the classical definition for transfer function of a negative-feedback closed loop control system (without the controller) in Equation (6), the numerical uncontrolled closed loop transfer function of the system is computed using MATLAB and it is given by Equation (7).

$$\frac{\theta_y(s)}{\theta_d(s)} = \frac{G_{amp}(s)\times G_a(s)\times G_{sat}(s)}{1+[G_{amp}(s)\times G_a(s)\times G_{sat}(s)]\times H(s)} \quad (6)$$

$$\frac{\theta_y(s)}{\theta_d(s)} = \frac{18792\,s}{0.08\,s^5 + 146\,s^4 + 3410\,s^3 + 1.957\times10^4 s^2 + 18792\,s} \quad (7)$$

where $\theta_d(s)$ is the desired attitude (target yaw angle), $\theta_y(s)$ is the actual attitude (current yaw angle), and $H(s)$ is the unity feedback gain of the measurement sensor.

Design of MRAC-PID Controller

A model reference adaptive controller (MRAC) is designed in this section. Several approaches are used in the design such as Lyapunov theory, augmented error theory and Massachusetts Institute of Technology (MIT) rule. In this paper, a MRAC is developed using the MIT technique. Designing the MRAC using MIT requires that the error and cost function be established as will be determined in subsequent subsections. The block diagram of the proposed system is shown in Figure 3.

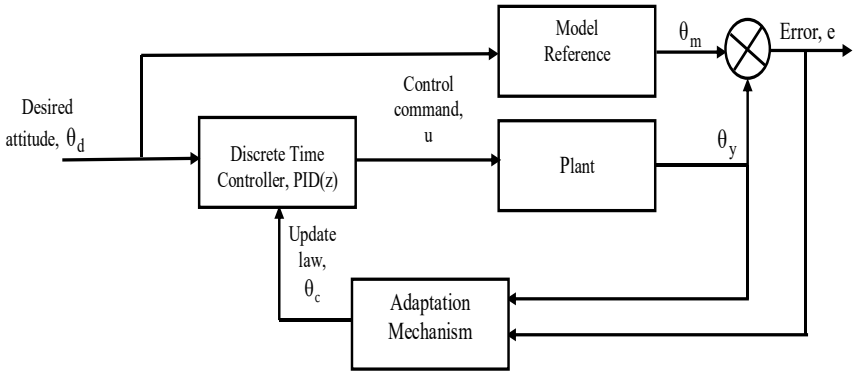


Figure 3. Block diagram of proposed microsatellite yaw-axis attitude control system

Adjustment mechanism

Let the difference between actual output of the process and the reference model θ_{model}output be defined as the error,e given by:

$$e = \theta_{\text{Actual}} - \theta_{\text{model}} \quad (8)$$

The cost function $\theta_c$is expressed in terms of the error in Equation (8) and is given by:

$$J(\theta_c) = \frac{1}{2}e^2 \quad (9)$$

Minimizing the cost function such that the change in the parameter $\theta_c$can be maintained in the direction of the negative gradient of J given by:

$$\frac{d\theta_c}{dt} = -\gamma \frac{\partial J}{\partial \theta_c} = -\gamma e \frac{\partial e}{\partial \theta_c} \quad (10)$$

Equation (10) is an expression of the change in $\theta_c$with respect to time in order to be able to minimize the cost function to zero (Eze *et al.*, 2017; Eze *et al.,* 2024). The expression $\partial e/\partial \theta_c$ is called the sensitivity derivative, which depicts the change in error *e* with respect to the cost function θ_c. The quantity γ is a positive value that represents the gain of the adaptation mechanism of the controller.

Now the objective is to design a reference model defined characteristic performance that the dished antenna position system will automatically follow or tracked irrespective of the variations in system or environment parameters.

Let the transfer function of the system be equal to $KG_p(s)$ where K is a parameter whose value is unknown. Also, let the reference model be approximated to a second order transfer function since the plant transfer function in Equation (1) is a second order model. Thus, the reference model is defined by:

$$G_m(s) = K_o G_p(s) \quad (11)$$

where K_o is a parameter, whose value is defined, thus the error, Equation (7) can be expressed by:

$$E(s) = KG_p(s)U(s) - K_o G_p(s)U_c(s) \quad (12)$$

where $KG_p(s)U(s) = \theta_{\text{Actual}}$ such that the control input to the plant is $U(s)$ and $K_o G_p(s)U_c(s) = \theta_{\text{model}}$ such that $U_c(s)$ is the control input to the reference model. Therefore, control law is state as given by:

$$U(s) = \theta_c \times U_c(s) \quad (13)$$

Substituting Equation (12) into Equation (11) and taking the partial derivative gives:

$$\frac{\partial E(s)}{\partial \theta_c} = \mathrm{KG}_p(s)U_c(s) = \frac{K}{K_o}\theta_{\mathrm{model}} \quad (14)$$

Equating Equation (10) and Equation (14) gives:

$$\frac{\mathrm{d}\theta_c}{\mathrm{dt}} = -\gamma \mathrm{e}\frac{K}{K_o}\theta_{\mathrm{model}} = -\gamma^{1}\mathrm{e}\theta_{\mathrm{model}} \quad (15)$$

where $\gamma^{1} = \gamma K/K_o$ and the Equation (15) is the law for parameter θ_c adjustment and represents the adjustment mechanism of the adaptive controller.

Reference Model

It is required that reference model $G_m(s)$ be designed approximately as a second order system similar to the dynamics of the satellite structure such that its transient and steady state performance meets the design criteria. Hence, the second order reference model is defined by:

$$G_m(s) = \frac{{\omega_n}^2}{s^2+2\zeta\varpi_n s+{\omega_n}^2} \quad (16)$$

where ω_n,ζ stands for the natural frequency and damping ratio. These quantities are determined as follows:

$$M_p = e^{-\pi\zeta/\sqrt{1-\zeta^2}} \quad (17)$$

where M_p is the maximum percentage overshoot of value 5%. Solving Equation (17) gives Equation (18):

$$\log_e\left(\frac{5}{100}\right) = -\frac{\pi\zeta}{\sqrt{1-\zeta^2}}\log_e^e \quad (18)$$

Solving (18) results in $\zeta = 0.69$ and taking a settling time of $T_s = 1$ s, the natural frequency of the system is computed using:

$$T_s = \frac{4}{\zeta\omega_n} \quad (19)$$

Thus, $\omega_n = 5.77$ rads^{-1}. Substituting these values into Equation (16) gives:

$$G_m(s) = \frac{33.29}{s^2+7.95s+33.29} \quad (20)$$

Equation (20) is the designed referenced model.

Design of discrete-time PID controller

The PID controller is the common controller largely used in industrial control systems for three-term closed loop feedback mechanism and it is shown in Figure 5.

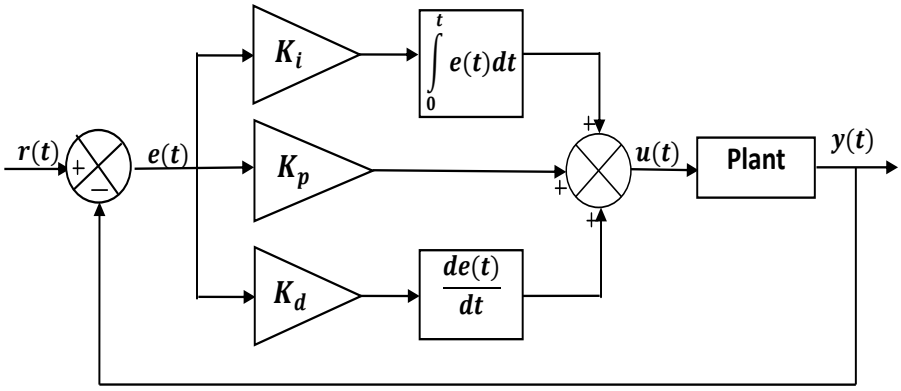


Figure 5. PID control system representation

The mathematical expression of PID controller can be determined by analyzing Figure 5. Hence, $r(t), e(t), u(t)$ represents the desired input, error and the control command. Furthermore, K_p, K_i, K_d are gains of the PID controller for proportional element, integral element, and derivative components, and y(t) is the output.

$$e(t) = r(t) - y(t) \quad (21)$$

The proportional, integral and derivative computation carried on the error as it is fed into the PID controller results to a control action given by Okoye et al. (2021):

$$u(t) = K_p e(t) + K_i \int_0^t e(t)\mathrm{dt} + K_d \frac{\mathrm{de}(t)}{\mathrm{dt}} \quad (22)$$

Equation (22) is an ideal PID controller in continuous time domain. Thus, the Laplace transform of PID control command assuming zero initial condition is given by:

$$U(s) = K_p E(s) + K_i \frac{1}{s} E(s) + K_d \mathrm{sE}(s) \quad (23)$$

Or in a simplified form as:

$$C(s) = K_p + K_i \frac{1}{s} + K_d s \quad (24)$$

where $C(s) = U(s)/E(s)$ and is the PID controller. The gains of the PID controller obtained by tuning the MATLAB/Simulink PID block are $K_p = 20.4, K_i = 0.0564$, and $K_d = 1.98$.

Having determined a suitable continuous time PID controller, a discrete time approximation operating at $1/T_s$ Hz (sampling time, T_s) is obtained using the forward Euler. Hence, a discrete time approximation to the continuous PID controller is given by:

$$C(z) = 20.4 + 0.0564\left(\frac{T_s}{z-1}\right) + 1.98\left(\frac{(z-1)}{T_s z}\right), \quad T_s = 0.02\ s \quad (25)$$

For the purpose of simulation, the sampling T_s is taken as 0.02 s.

Performance Specifications

The objective is to design an adaptive controller with approximated second order reference model based PID controller to meet the following tracking specifications expressed as maximum overshoot ($M_p \leq 5\%$), settling time ($t_s \leq 2$ s) with 2% criterion, zero steady-state error for a microstatellite yaw angle control system.

RESULTS

There are basically three subsections considered in this section to clearly analyse the obtained simulation results. These sections are simulation analysis of system without controller, simulation analysis of DPID, and simulation analysis of MRAC based DPID control system. The effectiveness of the control system is considered to be its ability to maintain or track a desired satellite yaw axis attitude which is taken in this paper as unit step input in degree while at the same time meeting the performance specifications.

Simulation analysis of system without controller

In this scenario, simulation analysis was conducted to investigate the performance of the microsatellite yaw axis attitude in the absence of a controller. That is no controller was introduced as a subsystem in the attitude control system (ACS) so as to ensure the stabilization of the satellite yaw angle and tracked the desired yaw-axis attitude while ensuring that the system performance criteria that include rapid convergence (that is reaching steady state as fast as possible, which is defined by the settling time in second)

with little or no cycling (defined in terms of peak overshoot in percentage) are met. The resulting step response of uncompensated satellite yaw-axis ACS is shown in Figure 6. The numerical analysis of the step response curve is shown in Table 1.

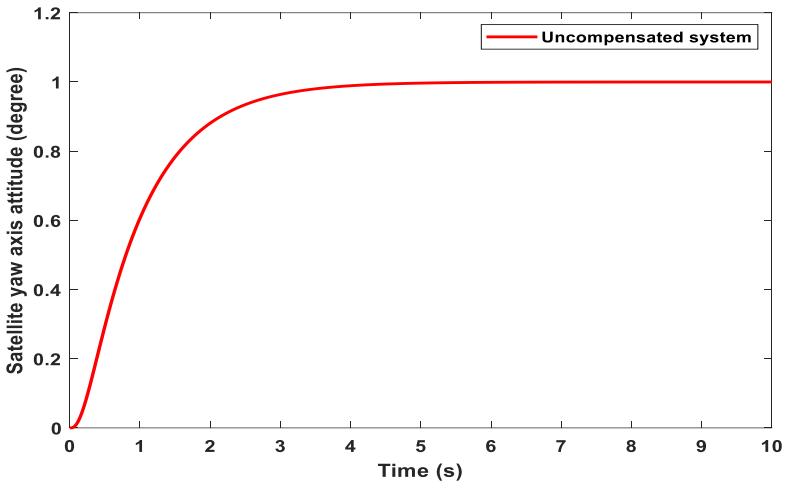


Figure 6.Step response of system without controller

Table 1. Time domain characteristics of system without controller

Step response parameter	value
Rise time	1.89 s
Transient time	3.49 s
Settling time	3.49 s
Peak overshoot	0
Peak time	10
Final value	1
Steady state error	0

Simulation analysis of system with discrete-time PID controller

This subsection presents the simulation scenario regarding the step response of the system when the discrete-time (DPID) controller was introduced as a subsystem into the ACS. The simulation plot is shown in Figure 7 and the numerical analysis is shown in Table 2.

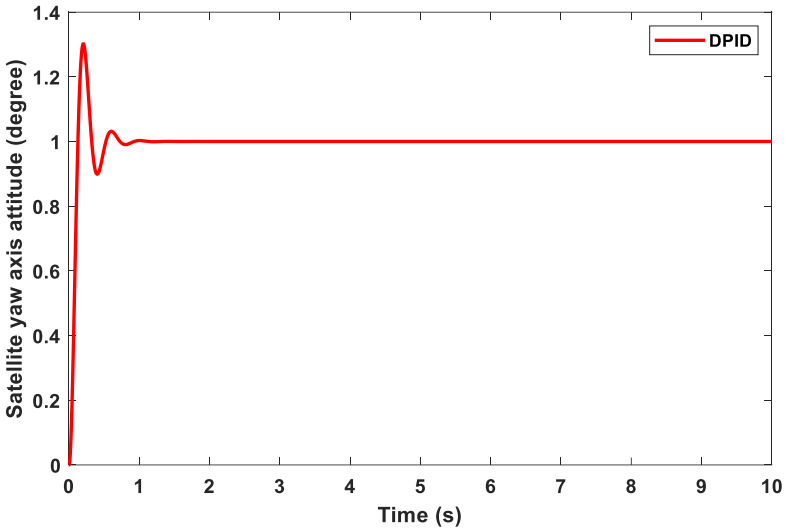


Figure 7. Step response of system with DPID controller

Table 2. Time domain characteristics of system with DPID controller

Step response parameter	value
Rise time	0.08 s
Transient time	0.66 s
Settling time	0.66 s
Peak overshoot	30.22%
Peak time	0.21
Final value	1
Steady state error	0

Simulation analysis of system with MRAC based DPID controller

The simulation results are presented in this section in terms of satellite yaw-axis attitude in degree for the MRAC-DPID proposed in this work that has wide adaptation gain (gamma) ranging from 0 to 20. The simulation plots are shown in Figures 8 and 9. In Figure 8, the step response plots of the system considering gamma from 0.1 to 1, while in Figure 9, the step response plots are presented for gamma ranging from 2 to 20. The numerical analysis of the step response plots in terms of transient and steady is shown in Table 3.

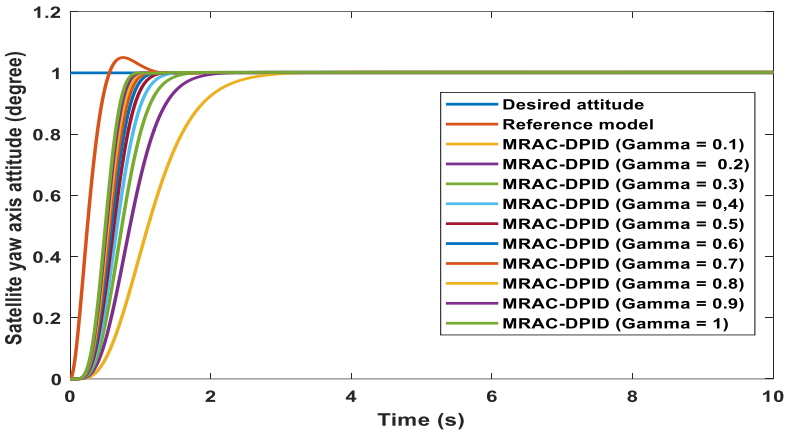


Figure 8. Step response of system with MRAC-DPID (gamma = 0.1 to 1)

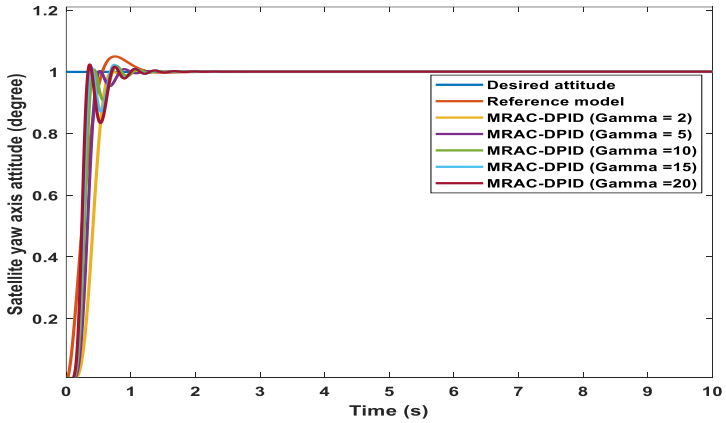


Figure 9. Step response of system with MRAC-DPID (gamma = 2 to 20)

Table 3. Step response characteristics of MRAC-DPID

System condition	t_r (s)	t_t (s)	t_s (s)	M_p (%)	t_p (s)	f_v	e_{ss}
MRAC-DPID (gamma = 0.1)	**1.32**	**2.54**	**2.54**	**0**	**5.92**	**1**	**0**
MRAC-DPID (gamma = 0.2)	0.90	1.77	1.77	0	3.96	1	0
MRAC-DPID (gamma = 0.3)	0.73	1.44	1.44	0	3.09	1	0
MRAC-DPID (gamma = 0.4)	0.63	1.25	1.25	0	2.68	1	0
MRAC-DPID (gamma = 0.5)	0.56	1.12	1.12	0	2.40	1	0
MRAC-DPID (gamma = 0.6)	0.51	1.03	1.03	0	2.11	1	0
MRAC-DPID (gamma = 0.7)	0.48	0.97	0.97	0	1.91	1	0

System condition	t_r (s)	t_t (s)	t_s (s)	M_p (%)	t_p (s)	f_v	e_{ss}
MRAC-DPID (gamma = 0.1)	**1.32**	**2.54**	**2.54**	**0**	**5.92**	**1**	**0**
MRAC-DPID (gamma = 0.8)	0.45	0.91	0.91	0	1.77	1	0
MRAC-DPID (gamma = 0.9)	0.42	0.87	0.87	0	1.67	1	0
MRAC-DPID (gamma = 1)	0.40	0.83	0.83	0	1.00	1	0
MRAC-DPID (gamma = 2)	0.30	0.64	0.64	0.12	1.19	1	0
MRAC-DPID (gamma = 5)	0.21	0.77	0.77	0.80	0.90	1	0
MRAC-DPID (gamma = 10)	0.17	0.69	0.69	1.86	0.78	1	0
MRAC-DPID (gamma = 15)	0.15	0.91	0.91	2.21	0.74	1	0
MRAC-DPID (gamma = 20)	0.13	0.92	0.0.92	2.31	0.36	1	0

where t_r is the rise time, t_t is the transient time, t_s is the settling time, M_p peak or maximum overshoot, t_p is the peak time, f_v is the final value, and e_{ss} is the steady state error.

However, looking at Figure 9, it can be observed that for adaptation gain 2 to 20, there is an associated oscillation (some sort of instability) associated with MRAC based DPID controller at the early stage of the control process which can adversely impact on the amplifier component of the microsatellite and thereby resulting in circuit being push into nonlinear region. This can lead to distortion in system performance and reduce efficiency. Figure 10 shows an in-depth view of the step response of the MRAC based DPID control system for the microsatellite yaw-axis attitude, which was achieved using the zoom in tool of the MATLAB linear time invariant (LTI) analysis.

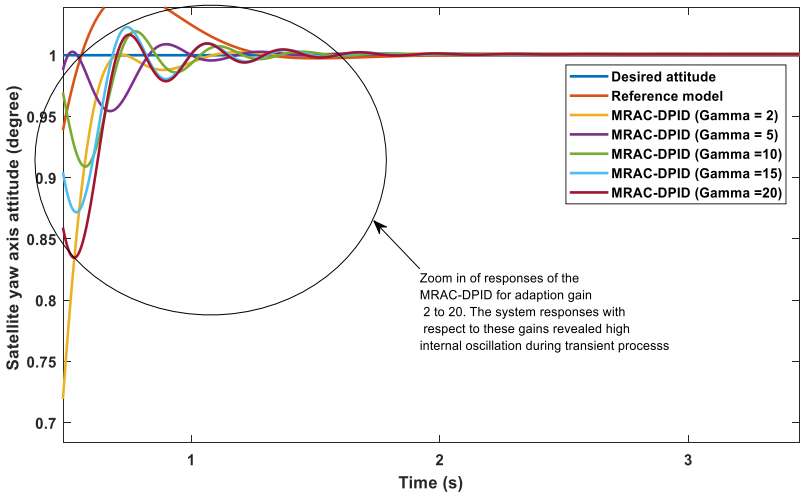


Figure 10. In-depth description of step responses of the MRAC-DPID (gamma = 2 to 20)

DISCUSSION

Considering the step response shown in Figure 6, the numerical analysis as shown in Table 1 revealed that in the absence of a control algorithm, the system has a transient and steady-state that is characterized by rise time of 1.89 s, transient time and settling time 3.49 s respectively, peak overshoot of 0, peak time of 10 s, final value of 1 degree, and steady state error of 0. As shown in Figure 6, the curve revealed that in the absence of a controller, the system response appears to be slow given the rise time and the fact that the system was not able to achieve the desired attitude at the predetermined convergence time (that is the stated settling time defined as the system performance criteria). Thus, there is need to design a controller for on-orbit flight performance improvement in terms of yaw angle.

Looking at Figure 7, it can be observed that step response of the DPID control system was initially subject to high oscillation resulting in high peak overshoot of 30.22% at time t = 0.21 s (peak time) as shown in Table 2. This is well above the required overshoot in terms of the performance specifications. However, except for the overshoot, the DPID meets every other performance criterion required of the system. Hence, there is need to address the associated high overshoot with the DPID controller.

Looking at Table 3 (representing performance parameters obtained from step responses of Figure8 and 9), it can be observed that the MRAC based DPID control system meets all the performance criteria of the design for all the adaptation gains except for 0.1 where the settling time was more than 2 s. However, despite the fact that for adaptation gains: 2 to 20, yielded promising performances in terms of the design criteria, the cycling associated with the control system responses as shown in Figure 10, can be detrimental to the operation of the ACS. Thus, the best performance of the proposed MRAC-DPID can be obtained for optimal gain of 0.2 to 1.

CONCLUSION

This paper has presented design of adaptive controller for microsatellite yaw-axis attitude control system (ACS). In order to realize the aim of this work, the dynamic equations representing the behaviour of a microsatellite yaw-axis in attitude control system were determined. A Model Reference Adaptive Control (MRAC) utilizing Discrete Proportional Integral and Derivative (DPID) controller (MRAC-DPID) was developed to

adaptively provide command action for microsatellite yaw-axis ACS. The proposed control system was modelled and simulated in MATLAB/Simulink environment. The MRAC-DPID offered a wide range of adaptation gains that can be used to provide adaptive technique for yaw-axis ACS. The tuning of the DPID controller to obtain adequate parameters was quite time consuming. Hence, a numerical selection based on trial and error method was used to select the DPID parameters after several simulation trials. The results from the simulation revealed that the proposed controller met the performance specifications of the microsatellite yaw-axis ACS particularly with adaptation gains from 0.2 to 20. However, best solution is for adaptation gains from 0.2 to 1.

REFERENCES

Agwah, B. C., & Eze, P. C. (2022). An intelligent controller augmented with variable zero lag compensation for antilock braking system. *International Journal of Mechanical and Mechatronics Engineering, 16*(11), 303–310.

Ajiboye, A. T., Popoola, J. O., Oniyide, O., & Ayinla, S. L. (2020). PID controller for microsatellite yaw-axis attitude control system using ITAE method. *TELKOMNIKA Telecommunication, Computing, Electronics and Control, 18*(2), 1001–1011. https://doi.org/10.12928/TELKOMNIKA.v18i2.14303

Bello, A., Olfe, K. S., Rodríguez, J., Ezquerro, J. M., & Lapuerta, V. (2023). Experimental verification and comparison of fuzzy and PID controllers for attitude control of nanosatellites. *Advances in Space Research, 71*(9), 3613–3630. https://doi.org/10.1016/j.asr.2022.05.055

Benzeniar, H., & Fellah, M. K. (2014). A microsatellite reaction wheel based on a fuzzy logic controller for the attitude control system. *International Review of Aerospace Engineering (IREASE), 7*(5), 171–176. https://doi.org/10.15866/irease.v7i5.4973

Dass, A. D., Sanusi, H., & Muad, A. M. (2019). Stabilizing roll, pitch and yaw angles for attitude control system (ACS) using direct torque control (DTC). *International Journal of Advanced Trends in Computer Science and Engineering, 8*(1.6), 263–267. https://doi.org/10.30534/ijatcse/2019/3981.62019

Enejor, E. U., Dahunsi, F. M., Akingbade, K. F., & Nelson, I. O. (2023). Low Earth orbit satellite attitude stabilization using linear quadratic regulator. *European Journal of Electrical Engineering and Computer Science, 7*(3), 17–29. https://doi.org/10.24018/ejece.2023.7.3.505

Eze, P. C., Ekengwu, B. O., Asiegbu, N. C., & Ozue, T. I. (2021). Adjustable gain enhanced fuzzy logic controller for optimal wheel slip ratio tracking in hard braking control system. *Advances in Electrical and Electronic Engineering, 19*(3), 231–242. https://doi.org/10.15598/aeee.v19i3.4124

Eze, P. C., & Ezenugu, I. A. (2024). Microsatellite yaw-axis attitude control system using model reference adaptive control based PID controller. *International Journal of Electrical and Computer Engineering Research, 4*(2), 8–16. https://doi.org/10.53375/ijecer.2024.389

Eze, P. C., Njoku, D. O., Nwokonkwo, O. C., Onukwugha, C. G., Odii, J. N., & Jibiri, J. E. (2024). Wheel slip equilibrium point model reference adaptive control based PID controller for antilock braking system: A new approach. *International Journal of Automotive and Mechanical Engineering, 21*(3), 11581–11595. https://doi.org/10.15282/ijame.21.3.2024.10.0893

Eze, P. C., Obichere, J. K., Mbonu, E. S., & Onojo, O. J. (2024). Positioning control of satellite antenna for high speed response performance. *IPTEK: The Journal of Engineering, 10*(2), 119–136. https://doi.org/10.12962/j23378557.v10i2.a20670

Eze, P. C., Ugoh, C. A., & Inaibo, D. S. (2021). Positioning control of DC servomotor-based antenna using PID tuned compensator. *Journal of Engineering Sciences, 8*(1), E9–E16. https://doi.org/10.21272/jes.2021.8(1).e2

Eze, P. C., Ugoh, C. A., Ezeabasili, C. P., Ekengwu, B. O., & Aghoghovbia, L. E. (2017). Servo position control in hard disk drive of a computer using MRAC integrating PID algorithm. *American Journal of Science, Engineering and Technology, 2*(4), 97–105. https://doi.org/10.11648/j.ajset.20170204.11

Okoye, U. P., Eze, P. C., & Oyiugo, D. C. (2021). Enhancing the performance of AVR system with prefilter aided PID controller. *Access International Journal of Research and Development, 1*(1), 19–32.